

Sequential Tunneling through Molecular Spin Rings

Jörg Lehmann and Daniel Loss

*Department of Physics and Astronomy, Universität Basel,
Klingelbergstrasse 82, CH-4056 Basel, Switzerland*

(Dated: February 6, 2008)

We consider electrical transport through molecules with Heisenberg-coupled spins arranged in a ring structure in the presence of an easy-axis anisotropy. The molecules are coupled to two metallic leads and a gate. In the charged state of the ring, a Zener double-exchange mechanism links transport properties to the underlying spin structure. This leads to a remarkable contact-site dependence of the current, which for an antiferromagnetic coupling of the spins can lead to a total suppression of the zero-bias conductance when the molecule is contacted at adjacent sites.

PACS numbers: 85.65.+h, 85.75.-d, 75.10.Jm, 73.63.-b

During the last decade, we have witnessed a tremendous progress in the experimental methods for contacting single molecules and measuring the electrical current through them [1–5]. A break-through has been achieved with the electromigration-junction technique [2], which allowed one to add a back-gate to the molecule, thereby bringing the whole field of Coulomb-blockade physics to molecular systems. Recently, this technique has led to the first transport measurements through single magnetic molecules: The current through the different Mn_{12} clusters [6] has been measured and magnetic excited states have been identified [3, 4]. At the same time, various theoretical models for the description of these measurements have been put forward, all based on the effective Hamiltonians routinely used for the description of thermodynamic properties of the molecular magnet [3, 4, 7–9]. Doing so, an immediate complication encountered is that for the description of the sequential tunneling processes observed in the experiment, at least one charged state of the molecule has to be included in the model, as well. As plausible models for this state, the effective Hamiltonian with renormalized parameters [3, 7] or modified by a single additional orbital [8] have been employed.

Here, we take a microscopic approach in terms of the constituent spins of the molecular magnet. Whereas this limits us to smaller systems than the ones considered experimentally, it enables us to include an excess charge. This will shed some light on the role of the orbital degree of freedom of this excess charge (say an electron) not contained in an effective-Hamiltonian model. Further, we are able to consider on the same footing transport through antiferromagnetically (AF) coupled rings like molecular ferric wheels [10], which has not been studied so far.

Evidently, an excess electron will reduce one of the positively charged ions forming the localized spins. The arbitrary choice of this ion leads to an orbital degeneracy which will, however, be lifted by a hopping process between the different sites. At the same time, this hopping allows the electron to travel from one side of the molecule to the other and a current to flow across the molecule. Since according to Hund's rules, the coupling of the excess electron to the localized spin will favor

one direction of the excess electron's spin, and assuming that hopping leaves the spin unchanged [17], one obtains an effective ferromagnetic (FM) type of coupling known as Zener double exchange [11]. Correspondingly, the orbital degree of freedom of the electron is linked with the spin structure of the ring. In particular for AF rings this should lead to interesting transport effects: Due to the Néel-ordered structure of the AF ground state, we even expect—and indeed confirm—a strong even-odd-site-dependence of the current mediated by ground-state transitions not present in the FM case. Another intriguing property of AF rings is that quantum tunneling of magnetization (QTM) leads to a tunnel-split ground-state doublet with a characteristic oscillating dependence on the magnetic field [12]. We will demonstrate how this behavior can be extracted in a transport measurement.

Model—The physical picture described in the previous paragraph is captured by the Hamiltonian

$$\begin{aligned}
 H_0 = & -J \sum_i \mathbf{S}_i \cdot \mathbf{S}_{i+1} - J_H \sum_i \mathbf{s}_i \cdot \mathbf{S}_i - k_z \sum_i (S_i^z + s_i^z)^2 \\
 & + g\mu_B (\mathbf{S} + \mathbf{s}) \cdot \mathbf{B} - t \left(\sum_{i,\sigma} d_{i,\sigma}^\dagger d_{i+1,\sigma} + \text{h.c.} \right) \\
 & + (\epsilon_0 - eV_g) n + Un(n-1)/2.
 \end{aligned} \tag{1}$$

Here, the first term describes the Heisenberg coupling between the localized spins \mathbf{S}_i with spin quantum number s , where we require periodic boundary conditions $\mathbf{S}_{N+1} = \mathbf{S}_1$ to describe a ring with total spin $\mathbf{S} = \sum_i \mathbf{S}_i$. The second term represents the Hund's rule coupling of the excess spin when it is localized at the site i to the corresponding spin \mathbf{S}_i . The second-quantized spin operators \mathbf{s}_i are defined in terms of the creation (annihilation) operators $d_{i,\sigma}^\dagger$ ($d_{i,\sigma}$) for an electron of spin σ at site i by $\mathbf{s}_i = (1/2) \sum_{\sigma\sigma'} \boldsymbol{\tau}_{\sigma\sigma'} d_{i,\sigma}^\dagger d_{i,\sigma'}$ with $\boldsymbol{\tau}$ being the vector of the three Pauli matrices. The spin of the excess electron is then given by $\mathbf{s} = \sum_i \mathbf{s}_i$. The easy-axis anisotropy of strength k_z and the Zeeman energy are included by the third and fourth term, respectively. The fifth term describes the hopping of the excess electron around the ring, where again periodic boundary conditions are assumed. The orbital energy ϵ_0 of the excess electron can

be tuned by applying an external gate voltage V_g and is proportional to the occupation number $n = \sum_i d_{i,\sigma}^\dagger d_{i,\sigma}$. Finally, we restrict ourselves to a single excess electron by letting the charging energy $U \rightarrow \infty$.

The coupling of the molecule to the metallic leads is described by the tunnel Hamiltonian $H_T = \sum_{\ell\mathbf{k}\sigma} T_{\ell\mathbf{k}} c_{\ell\mathbf{k}\sigma}^\dagger d_{i_\ell\sigma} + \text{h.c.}$ Here, the sum runs over the two leads $\ell = \text{L, R}$, which we assumed to be each coupled via a spin-independent coupling matrix elements $T_{\ell\mathbf{k}}$ to a single ring site i_ℓ . The leads at an electro-chemical potential μ_ℓ are modeled as a set of independent quasiparticles with wave-vector \mathbf{k} and spin σ , $H_L = \sum_{\ell\mathbf{k}\sigma} \epsilon_{\ell\mathbf{k}} c_{\ell\mathbf{k}\sigma}^\dagger c_{\ell\mathbf{k}\sigma}$, distributed according to the Fermi distribution $f(\epsilon - \mu_\ell) = \{1 + \exp[(\epsilon - \mu_\ell)/kT]\}^{-1}$. Assuming that the externally applied bias voltage V_b drops completely and symmetrically along both molecule-lead contacts, we have $\mu_{\text{L,R}} = \mu \pm eV_b/2$, where μ is the Fermi energy.

Magnetic order—The eigenstates $|\alpha\rangle$ of the unperturbed ring Hamiltonian (1) can be separately considered for the cases of an uncharged ($n = 0$) and charged ($n = 1$) ring. Moreover, the discrete translational symmetry and the symmetry of reflection at an arbitrary site, say $i = 1$, yield corresponding good quantum numbers $\cos(q)$ with $-\pi < q \leq \pi$ and $Nq = 0 \bmod 2\pi$, and parity $P = \pm 1$, respectively. In the absence of a magnetic field with x - and y -components, another good quantum number M is given by the z -component of the total angular momentum $\mathbf{S} + \mathbf{s}$. The transition matrix elements $\langle \alpha' | d_{i,\sigma}^\dagger | \alpha \rangle$ of the creation operator fulfil the selection rules $n' - n = 1$ and $M' - M = \sigma$. In the special case $N = 4$ considered below, we find $P' = P$ for odd site numbers $i = 1, 3$ and $\exp(2iq')P' = \exp(2iq)P$ for even site numbers $i = 2, 4$.

We now discuss the magnetic order of the lowest-lying states for the two opposite cases of a FM and AF intraring coupling J . In both cases, we assume that the ions forming the localized spins have at least half-filled shells and thus consider according to Hund's rules a strong AF coupling $J_H \ll -|J|$. This describes, for instance, ferric wheels containing Fe^{3+} ions. We will exemplify the general discussion by the special case of a ring consisting of $N = 4$ spins $s = 1$ (cf. Fig. 1). The exchange coupling strength $|J|$ serves as energy unit (typical values for ferric wheels range from 20 to 30 $k_B\text{K}$ [10]). The anisotropy is set to $k_z = 0.3|J|$ and the Hund's rule coupling strength is $J_H = -100|J|$. An estimate for the hopping matrix element t is difficult to make. Assuming that it is of the same order of magnitude as the one leading to exchange in the uncharged ring, a simple argument based on a Hubbard model yields the lower bound $J/4t \approx t/U' \ll 1$, where U' is the on-site charging energy. Expecting the excess electron to be rather localized, we assume $t = 5|J|$.

For a FM intra-ring coupling, the lowest-lying states of both the neutral and charged ring consist of multiplets of total spin $S = Ns$ and $S = Ns - 1/2$, respectively [cf. Fig. 1(a)]. These multiplets are split by the easy-axis anisotropy into doublets with same absolute value of the magnetic quantum number $|M|$. The additional FM-type

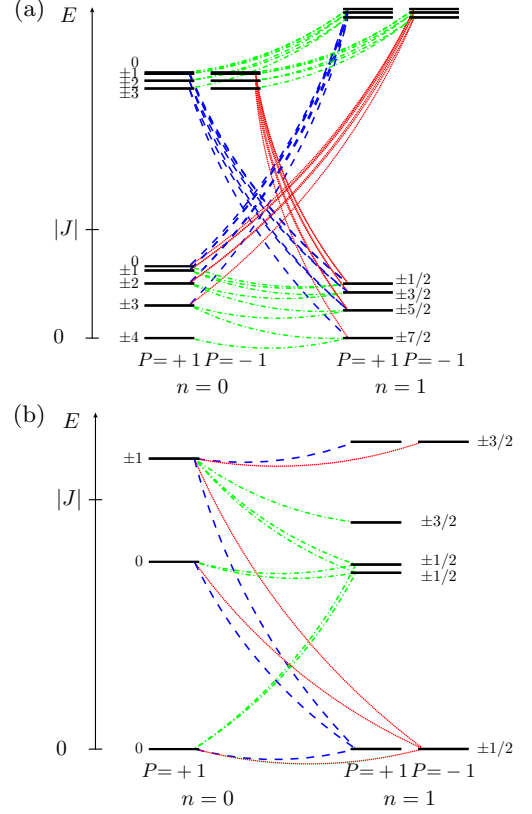


FIG. 1: (Color online) Low-energy states of the neutral (left, $n = 0$) and charged (right, $n = 1$) ring both for (a) FM and (b) AF coupling. The parameters are given in the main text. The levels are labeled by their magnetic quantum number M and their parity P . Dashed (dotted) lines indicate tunnel transitions allowed when the ring is contacted at the odd (even) numbered sites. Transitions allowed for all contact sites are drawn as dash-dotted lines.

interaction due to the Zener double exchange influences the magnetic order only weakly.

This is in stark contrast to the case of an AF intraring coupling $J < 0$ [cf. Fig. 1(b)], which, for the charged ring, competes with the double-exchange contribution. In order to understand the resulting magnetic ordering in this case, we first consider the *uncharged* ring. The classical ordering is described by the two Néel states $|\uparrow\rangle = |s, -s, s, -s, \dots\rangle$ and $|\downarrow\rangle = |-s, s, -s, s, \dots\rangle$, where the vectors have been written in the $\{S_{z,i}\}$ eigenbasis. In the QTM regime defined by the scaled tunnel action $S_0/\hbar = Ns\sqrt{2k_z/J}$ being much larger than unity [12], the leading contribution to the two lowest-lying quantum-mechanical eigenstates of the uncharged ring is then given by the symmetric and antisymmetric superposition of the two Néel states, i.e., $(|\uparrow\rangle \pm |\downarrow\rangle)/\sqrt{2}$.

Similarly, in a purely classical picture and without hopping contribution, the *charged* ring has a $2N$ -fold degenerate ground state which for an AF on-site coupling $J_H < 0$ consists of the states $|\uparrow\rangle|i, \uparrow\rangle$ and $|\downarrow\rangle|i, \downarrow\rangle$ for odd i

as well as $|\uparrow\rangle|i, \downarrow\rangle$ and $|\downarrow\rangle|i, \uparrow\rangle$ for even i . Here, $|i, \sigma\rangle$ describes the state of the excess electron being localized at site i with spin σ . The hopping leads to an hybridization of the states of same Néel ordering and excess electron spin. Furthermore, QTM couples states with opposite Néel ordering of the localized spin lattice.

We find for the special case with $N = 4$ and $s = 1$ [cf. Fig. 1(b)] that the ground and first excited state of the uncharged ring are indeed dominated by the superposition of the Néel-ordered states described above. The ground state of the charged ring turns out to be four-fold degenerate, discerning into two degenerate Kramers doublets with $M = \pm 1/2$. Focusing on the states with $M = 1/2$, we find that in the parity (P) eigenbasis, the main contribution to the eigenstates stems from the states $|\uparrow\rangle(|2, \uparrow\rangle - |4, \uparrow\rangle)$ with positive parity $P = 1$ and $|\downarrow\rangle(|1, \uparrow\rangle - |3, \uparrow\rangle)$ with negative parity $P = -1$. These states do not exhibit a QTM-induced tunnel splitting [18]. The situation is different for the two next excited Kramers doublets. The leading contribution to these states is given by the symmetric and antisymmetric combination of the two states $|\uparrow\rangle(|1, \uparrow\rangle + |3, \uparrow\rangle)$ and $|\downarrow\rangle(|2, \uparrow\rangle + |4, \uparrow\rangle)$ and we indeed observe a finite tunnel-splitting due to QTM.

Bloch-Redfield approach—We calculate the sequential-tunneling current through the ring using a Bloch-Redfield approach, extending previous results [13]. In contrast to a Pauli master-equation description, this includes off-diagonal elements (coherences) of the reduced density-matrix $\varrho_{\alpha\beta} = \text{Tr}_L \langle \alpha | \varrho | \beta \rangle$ after tracing out the leads and is also valid for level spacing less than the level broadening induced by the leads. We find

$$\dot{\varrho}_{\alpha\beta} = -i\omega_{\alpha\beta}\varrho_{\alpha\beta} + \frac{1}{2} \sum_{\ell\alpha'\beta'} \left\{ [W_{\beta'\beta\alpha\alpha'}^\ell + (W_{\alpha'\alpha\beta\beta'}^\ell)^*] \varrho_{\alpha'\beta'} - W_{\alpha\beta'\beta'\alpha'}^\ell \varrho_{\alpha'\beta} - (W_{\beta\alpha'\alpha'\beta'}^\ell)^* \varrho_{\alpha\beta'} \right\}. \quad (2)$$

Here, we have introduced the frequencies $\omega_{\alpha\beta} = (E_\alpha - E_\beta)/\hbar$ and the transition rates $W_{\beta'\beta\alpha\alpha'}^\ell = W_{\beta'\beta\alpha\alpha'}^{\ell+} + W_{\beta'\beta\alpha\alpha'}^{\ell-}$ due to tunneling across a molecule-lead contact ℓ in terms of the rates $W_{\beta'\beta\alpha\alpha'}^{\ell+} = \Gamma_\ell(E_\alpha - E_{\alpha'}) f(E_\alpha - E_{\alpha'} - \mu_\ell) \sum_\sigma \langle \beta' | d_{i_\ell, \sigma} | \beta \rangle \langle \alpha | d_{i_\ell, \sigma}^\dagger | \alpha' \rangle$ and $W_{\beta'\beta\alpha\alpha'}^{\ell-} = \Gamma_\ell(E_{\alpha'} - E_\alpha) [1 - f(E_{\alpha'} - E_\alpha - \mu_\ell)] \sum_\sigma \langle \beta' | d_{i_\ell, \sigma}^\dagger | \beta \rangle \langle \alpha | d_{i_\ell, \sigma} | \alpha' \rangle$ for tunneling of an electron on and off the molecule, where $\Gamma_\ell(\epsilon) = (2\pi/\hbar) \sum_{\mathbf{k}} |T_{\ell\mathbf{k}}|^2 \delta(\epsilon - \epsilon_{\ell\mathbf{k}})$ is the spectral density of the coupling. Finally, the current across contact ℓ is given by $I_\ell = e \text{Re} \sum_{\alpha\alpha'\beta} (W_{\beta\alpha'\alpha'\alpha}^\ell - W_{\ell\beta\alpha'\alpha}^{\ell+}) \varrho_{\alpha\beta}$.

The number of rates $W_{\beta'\beta\alpha\alpha'}^\ell$ scales with the fourth power of the dimension of the molecular Hilbert space. For the numerical solution of Eq. (2), we thus cannot take into account all coherences. However, for the stationary solution, coherences between states with an energy difference much larger than the molecule-lead coupling strength are negligible.

Differential conductance—For our numerical calcula-

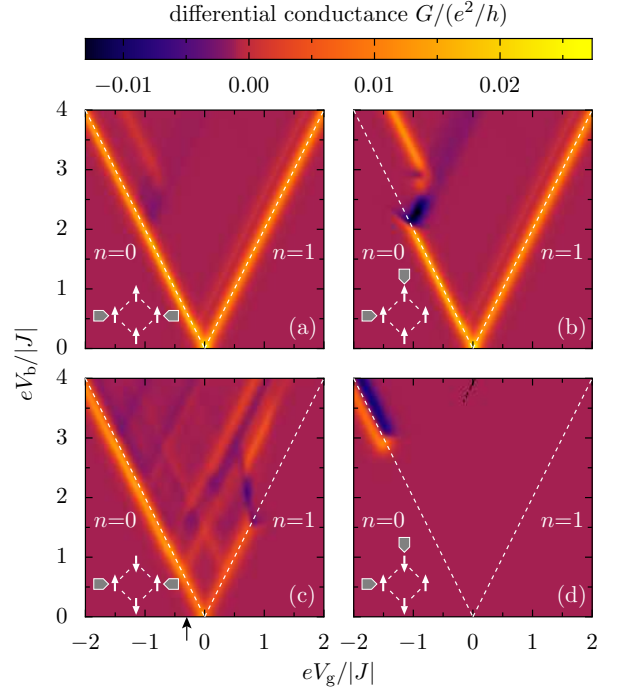


FIG. 2: (Color online) Differential conductance (color-coded) as a function of gate and bias voltage at zero magnetic field. The temperature is $k_B T = 0.05|J|$ and the other parameters are as given in the main text. The upper two panels (a) and (b) show the conductance for an FM coupling $J > 0$, the lower panels (c) and (d) depict the AF situation $J < 0$. The left (right) panels show the conductance when the molecule is contacted at opposite (adjacent) sites $i_L = 1$ and $i_R = 2$ ($i_L = 1$ and $i_R = 3$) (cf. inset schematic drawings). The dashed lines indicate the position of the ground-state transitions.

tions, we use the model parameters described above and assume a contact- and energy-independent molecule-lead coupling $\hbar\Gamma = \hbar\Gamma_\ell = 0.01|J|$. Figure 2 shows the differential conductance $G = dI/dV_b$ as a function of bias and gate voltage at zero magnetic field for both the FM and the AF case and for two molecule-lead coupling variants: contacts at *opposite* and *adjacent*, respectively, sides of the ring. For a FM coupling $J > 0$, the behavior in the low-bias-voltage regime is identical in both cases [see Figs. 2(a) and (b)]: the ground-state transitions dominate the current and one excited state can be identified. Away from the charge-degeneracy point, one ground-state transition is suppressed for adjacent contacts, for reasons similar to the AF case discussed next [14].

In the case of an AF intra-ring coupling $J < 0$, we find a more striking difference between the two contacting situations. For adjacent contacts [see Fig. 2(d)], *the low-bias conductance is completely suppressed*, which does not occur for contacts at opposite sides [see Fig. 2(c)]. In order to understand this remarkable difference, we consider the magnetic order discussed above. There, we identified two Kramers doublets of different parity in the $n = 1$ ground state. Furthermore we found the contact-site de-

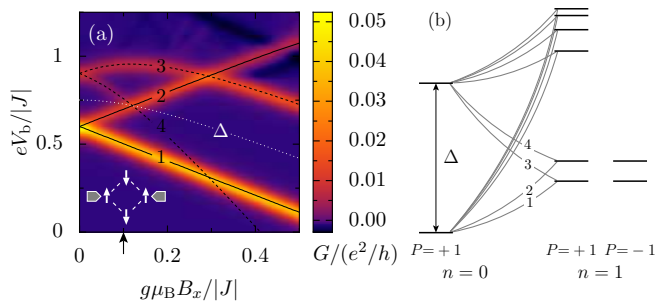


FIG. 3: (Color online) (a) Differential conductance through an AF coupled ring contacted at opposite sides as a function of magnetic field in x -direction and bias voltage. The gate voltage has been chosen as indicated by the arrow in Fig. 2(d). The temperature is $k_B T = 0.01|J|$ and the other parameters are given in the main text. The solid (dashed) lines indicate the electron (hole) transition labeled in panel (b). The tunnel splitting Δ extracted from these transitions is shown as white dotted line. (b) Level structure of the ring and tunnel transitions for finite B_x as indicated by the arrow in panel (a).

pendent selection rules depicted in Fig. 1. In particular, when contacting at adjacent sites, one contact only allows transitions to the even parity states and the other one only to the ones with odd parity. Thus, there is no transport path connecting both contacts and the current is blocked completely until transitions via excited states become possible at higher bias-voltages. On the other hand, for contacts at opposite sides, only one parity state becomes populated and a current can flow. It displays a rather complex excited-state spectrum compared to the FM case. For a better understanding of this regime, we focus on a fixed gate voltage as indicated by the arrow in Fig. 2(c) and consider in Fig. 3(a) the conductance as a function of an in-plane magnetic field. This

dependence is particularly interesting for AF rings where the QTM-induced tunnel splitting Δ between ground and first excited state of the neutral ring [see Fig. 3(b)] oscillates as a function of the magnetic field [12]. In order to extract this splitting from the conductance behavior, we identify all transitions between the lowest-lying states of the neutral and charged molecule (see labeled lines in Fig. 3). Denoting the magnetic-field dependent bias voltages at the corresponding resonances by $V_{b,k}$ ($k = 1, \dots, 4$), the tunnel splitting can be obtained as $\Delta = e(V_{b,1} + V_{b,3})/2 = e(V_{b,2} + V_{b,4})/2$.

We finally remark that a similar contact dependence of the current, albeit not a complete suppression of the zero-bias conductance, has been predicted for benzene rings [15]. There, it was also noted that when excited states are populated, a non-tunneling decay may lead to a population of the odd-parity state such that for contacts at opposite sides one may find a current collapse at higher bias voltages. A similar scenario can be envisaged here with the additional possibility to lift the blockade again by applying a large-enough magnetic field B_x [14]. Then, the current should display an interesting hysteric behavior possibly useful for information storage purposes.

To conclude, we have presented a model for a molecular spin ring in the presence of a single excess electron. It contains a hopping term which both provides a transport path and results in a Zener double-exchange coupling between the localized spins. For AF coupled rings of ions with least half-filled shells, the interplay of these two effects leads to a strong contact-dependence of the sequential tunneling current through the molecule reflecting the Néel-ordered ground states.

We thank D. Bulaev, W.A. Coish, J. Egues, and M. Wegewijs for discussions. Financial support by the EU RTN QuEMolNa, the NoE MAGMANet, the NCCR Nanoscience, and the Swiss NSF is acknowledged.

-
- [1] *Molecular Electronics, Lecture Notes in Physics*, edited by G. Cuniberti, G. Fagas, and K. Richter (Springer, Berlin, 2005).
 - [2] H. Park *et al.*, Appl. Phys. Lett. **75**, 301 (1999).
 - [3] H. B. Heersche *et al.*, Phys. Rev. Lett. **96**, 206801 (2006).
 - [4] M.-H. Jo *et al.*, Nano Lett. **6**, 2014 (2006).
 - [5] C. F. Hirjibehedin, C. P. Lutz, and A. J. Heinrich, Science **312**, 1021 (2006).
 - [6] R. Sessoli *et al.*, Nature (London) **365**, 141 (1993).
 - [7] C. Romeike, M. R. Wegewijs, and H. Schoeller, Phys. Rev. Lett. **96**, 196805 (2006).
 - [8] C. Timm and F. Elste, Phys. Rev. B **73**, 235304 (2006).
 - [9] M. N. Leuenberger and E. R. Mucciolo, Phys. Rev. Lett. **97**, 126601 (2006).
 - [10] K. L. Taft *et al.*, J. Am. Chem. Soc. **116**, 823 (1994); A. Caneschi *et al.*, Chem. Eur. J. **2**, 1379 (1996); M. Affronte *et al.*, Phys. Rev. B **60**, 1161 (1999); B. Normand *et al.*, *ibid.* **63**, 184409 (2001); A. Honecker *et al.*, Eur. Phys. J. B **27**, 487 (2002).
 - [11] C. Zener, Phys. Rev. **82**, 403 (1951); P. W. Anderson and H. Hasegawa, *ibid.* **100**, 675 (1955).
 - [12] A. Chiolero and D. Loss, Phys. Rev. Lett. **80**, 169 (1998).
 - [13] H.-A. Engel and D. Loss, Phys. Rev. Lett. **86**, 4648 (2001); S. Kohler, J. Lehmann, and P. Hänggi, Phys. Rep. **406**, 379 (2005).
 - [14] Details will be presented elsewhere.
 - [15] M. H. Hettler *et al.*, Phys. Rev. Lett. **90**, 076805 (2003).
 - [16] D. Loss, D. P. DiVincenzo, and G. Grinstein, Phys. Rev. Lett. **69**, 3232 (1992); J. von Delft and C. L. Henley, *ibid.* **69**, 3236 (1992); M. N. Leuenberger and D. Loss, Phys. Rev. B **63**, 054414 (2001).
 - [17] For simplicity, we disregard spin-orbit-interaction induced spin flips during the hopping process.
 - [18] We speculate that a physical interpretation might be given in terms of a geometrical-phase effect [16]. However, this needs further investigation.